

THE OSAKA UNIVERSITY RCNP 230-cm ISOCHRONOUS CYCLOTRON

M. Kondo, I. Miura, T. Yamazaki, H. Ejiri, A. Shimizu, M. Inoue, K. Hosono, T. Saito, Y. Nagai, H. Sakai, N. Matsuoka and S. Yamabe

Research Center for Nuclear Physics, Osaka University, Suita, Osaka, Japan.

Abstract

This paper describes the design, construction, performance and operation of the 230-cm cyclotron at Research Center for Nuclear Physics (RCNP). The design and construction of the machine were started in 1971. The first internal beam was obtained in July 1974 and the extracted beam was transported to the experimental area in August 1975.

1. Introduction

This cyclotron is designed to accelerate protons up to 75 MeV, deuterons up to 60 MeV,  $^3\text{He}$  particles up to 150 MeV and  $^4\text{He}$  particles up to 120 MeV. Also is possible to accelerate heavy ions, and polarized protons and deuterons. Many efforts have been made to get stable and high quality beam.

2. Magnet System

The main magnet assembly consists of the magnet core, poles, pole tips and shims, and flanges of the vacuum chamber. The magnet core consists of upper and lower yokes and two side yokes. Each yoke is made of laminated carbon steel sandwiched by killed steel. The overall dimensions of the magnet core are 6,300 mm  $\times$  3,850 mm  $\times$  2,540 mm. The total weight of the magnet is approximately 400 tons. The ion source drive mechanism which resembles to the Berkeley 88 in. machine's is installed at the bottom of the magnet yoke. The poles are made of forged low carbon steel and the pole tips and shims are made of forged pure iron with a carbon content of 0.008%. The flanges of the vacuum chamber are welded to the pole tips. Three flat spiral shims are equally spaced about the pole tip center. The maximum spiral angle of the magnetic field is 57 degrees at the 13 kG field level. The hill gap and valley gap are 206.6 mm and 347 mm, respectively.

The copper conductor with a cross section of 24 mm square is used for the main coil. It has a 16-mm diameter hole at the center of the conductor for water cooling. The main coil produces  $6 \times 10^5$  ampere-turns. Each of the upper and lower tanks of the main coil contains an auxiliary coil. The total weight of copper is approximately 15 tons. The sixteen separate pairs of concentric circular trim coils are used to control radial profile of the magnetic field. There are five pairs of valley coils in each valley. These valley coils are capable of producing the first harmonic field with any phase and amplitude up to 20 G without changing the azimuthally averaged field. The hollow mineral-insulated (MI) cable of the trim coil and the solid MI cable of the valley coil have been brazed to the base plate without using any flux in hydrogen atmosphere. The schematic view of the magnet assembly is shown in fig. 1.

The maximum rating currents of the power supplies are 1,430 A for the main coil, 750 A or 1,500 A for

the trim coil and 100 A or 200 A for the valley coil. The power supplies of the main coil and the trim coil are pre-regulated by a motor generator and a saturable reactor, respectively. All the power supplies are current regulated by series transistors with a stability of  $1 \times 10^{-5}/\text{h}$  for the main coil,  $1 \times 10^{-4}/\text{h}$  for the trim coil, and  $1 \times 10^{-3}/\text{h}$  for the valley coil. A d.c. current transformer is used as a current sensor of the trim coil power supply.

The magnetic field has been measured mostly by using a large rotating gear system with a Hall probe SIEMENS FC33. The radial and azimuthal positionings have been accurate to 0.1 mm and 10 seconds, respectively. The output of the probe has been measured by a five-decade digital voltmeter and punched out. The measurement accuracy of the whole system has been  $1 \times 10^{-4}$  in a few months. The off-median plane maps have been made using the Hall probe moved upward and downward by 10 mm from the geometrical mid plane. The axial hole field at the center has been measured by an axial type Hall probe. The results of the measurement of the magnetic field show good performance which has been expected from the model-magnet tests. An example of the predicted and measured magnetic fields is shown in fig. 2.

3. RF System

A  $1/4 \lambda$  mode coaxial resonator with a sliding short is chosen for its simplicity and an economy of RF power. The resonance frequency is variable from 5.5 MHz to 19.5 MHz. The coaxial cavity is fabricated from copper-clad steel plates. The inner and the outer diameter of the coaxial cavity are 1 m and 2.5 m, respectively. The shorting current at 19.5 MHz is estimated to be 13 kA (peak) for a 100 kV (peak) excitation. The sliding short has 288 inner and 660 outer silver contacts. Each contact is mounted on an end of 96 comblike water cooled chrome copper leaf springs. Each contact is directly connected to the shorting plate with 0.1 mm thick copper foils. The contacts are pushed by atmospheric pressure through 24 bellows. The forces on each inner and each outer contacts are 2 kg and 1 kg, respectively. The measured Q values for 5.5 MHz and 19.5 MHz are 12,000 and 4,400, respectively. The RF power is expected to be 130 kW for the 100 kV (peak) excitation at 19.5 MHz. The RF power is fed into the resonator through capacitive coupling. The load impedance can be adjusted from 150  $\Omega$  to 300  $\Omega$ .

The accelerating electrodes consist of a 180° single dee, a dummy dee, a dee insert, a dummy dee insert and a movable puller. The beam aperture of the dees and inserts are 44 mm and 10 mm, respectively. A box structure dee frame is fabricated from stainless steel and covered with water cooled OFHC-copper sandwich plates.

A MOPA system is developed for the RF system. The system is divided into five major components; an Anritsu MG417B frequency synthesizer, a modulator, a band pass filter (5 ~ 20 MHz), a driver amplifier (Marconi H-1000) and a final amplifier. The schematic diagram of the amplifier is shown in fig. 3. An RCA 4648 tetrode is used as a class AB<sub>1</sub> linear amplifier in the final amplifier. This amplifier is able to deliver 200 kW RF power to the resonator, which is sufficient to produce 120 kV (peak) on the dee at 19.5 MHz. A symmetric  $\pi$  network input circuit consists of a Lecher line with a sliding short, the input

capacity of the 4648 and a 1,200 pF vacuum capacity. The ends of the Lecher line are connected together at the another side and grounded through a  $10 \Omega$  damper resistance. No resonance was observed except the normal mode up to 100 MHz. The output of the driver amplifier is fed to a branch of the  $\pi$  network through a  $50 \Omega$  cable 30 m in length and terminated on the another branch with a 1 kW water cooled  $50 \Omega$  damper. The anode load impedance of the 4648 was measured continuously from 0.5 MHz to 100 MHz as a function of length of the cavity. The results of the measurement are shown in fig. 4. Three dampers and the band pass filter are inserted to increase stability and to reduce the harmonic voltage on the dee and the RF power feeder. The screen bypass capacitor of  $0.03 \mu\text{F}$  is formed by a double sandwich disk of 5-mil Kapton films and copper plates. The final amplifier is working in very stable condition without neutralization. Highly stabilized power supplies are used for the final amplifier. The noise level of the dee voltage is about  $2 \times 10^{-3}$  peak to peak noise per peak RF voltage without a dee voltage stabilizer. The main noise is 60 Hz originated in the driver amplifier.

This MOPA system has an automatic tuning system and a dee voltage stabilizer. The d.c. stability and the noise levels of the dee voltage are  $10^{-4}$  (p-p)/p on no beam-loading condition. No effect of beam-loading was observed for the d.c. stability. But, the noise levels increase evidently depending on the loading. Most of the noise is distributed around 10 kHz. A new dee voltage detector which is insensitive to the dee motion, and a new wide band feedback amplifier are being developed. Pulse modulated dee voltages and pulsed beams (100 p/sec) are obtained, using a pulsed reference voltage.

#### 4. Vacuum System

The vacuum chamber consists of a  $3 \text{ m} \times 3.7 \text{ m} \times 0.6 \text{ m}$  square accelerating chamber and a  $2.5 \text{ m ID} \times 4.5 \text{ m}$  long dee stem tank. The former is composed by stainless steel plates and demountable by use of three way seal. Viton is used for elastmer seal.

Two 36 in. pumps at the accelerating chamber and a 22 in. pump at the rear of dee stem tank both with the refrigerated double chevron baffles evacuate the whole system. Each is backed by the series of a small diffusion pump, mechanical booster and Kinney pump. The effective pumping speed for air on the top of the baffle is 12,000  $\ell/\text{sec}$  and 4,000  $\ell/\text{sec}$  for 36 in. and 22 in. pump systems respectively. The pump fluid is "Lion S" whose main component is monoalkyl naphthalene. Backstreaming is carefully removed by the design of top nozzle and baffles. A roughing system is of a 2,400  $\text{m}^3/\text{h}$  mechanical booster and two 6,000  $\ell/\text{min}$  Kinney pumps. The Kinney pumps evacuate the  $25 \text{ m}^3$  vacuum system from air to 10 Torr in about 20 min and the booster pumps down to  $1 \times 10^{-3}$  Torr in another 20 min. Automatic operation of the whole system is possible on the control panel.

An operation pressure is  $5 \times 10^{-7}$  Torr at the top of the baffle and  $1.5 \times 10^{-6}$  Torr at the chamber wall, respectively, with normal gas load.

#### 5. Cooling System

The primary cooling system circulates clean and demineralized water at typical pressure of  $4 \text{ kg}/\text{cm}^2$  to cool down the machine. The system is divided into

five separate loops. The low conductivity water is supplied by a mixed-bed demineralizer and a slip stream is recycled through the demineralizer cartridges to keep the conductivity less than 3 micromho for appropriate loops. More than 150 return pipings of copper are separately settled for respective equipments between cyclotron vault and pump station site where one has access to in machine operation. The individual flow rates meters which have tapered stainless steel floats and adjacent switches for interlock system are placed at this site. Cooling towers are set on the roof of building to cool the primary water through the plate type heat exchangers. Chillers back up them to cool primary system in hot season.

#### 6. Ion Source and Gas System

The Livingston-type ion source is installed axially in the lower yoke. A hair pin type filament is fabricated from 2.8 mm  $\phi$  tungsten wire. The length of the hair pin and the center distance between both ends are 30 mm and 10 mm, respectively. The both ends are clamped with a single 4 mm  $\phi$  screw. This ion source is used with filament currents of 300 A and is operated without serious bending of the filament in the maximum magnetic field.

The current stability of the d.c. filament power supply and the a.c. input voltage stability of the arc power supply are  $10^{-3}$ . Using the regulated power supplies, extremely stable beams are obtained. A conical ion exit slit 2 mm in diameter is used throughout the initial operation to reduce beam currents and activations. The PIG type heavy ion source is under development. The Westinghouse WL-23219B control diode is used as a series regulator for an arc power supply of the heavy ion source.

The ion source gas system provides with six different gases. The bottles, regulators and manually-operated valves are located outside the vault. Variable leak-rate valve, Pirani gauge, electrically-operated valves are mounted below the main magnet. These are remotely controlled. The gas change is operated at the site of gas bottles.

A  $^3\text{He}$  recovery system with charcoal trap is also located outside the vault. Two sealed 350  $\ell/\text{min}$  rotary pumps are set; one is at the direct back of the mechanical boosters of the 36 in. diffusion pump systems and the other is at the back of the charcoal trap. The operating pressure at the trap is about 10 Torr. A test of the system with  $^4\text{He}$  gas has been successfully performed.

#### 7. Axial Ion-injection System

An axial ion-injection system for external ion sources has been designed and constructed. The polarized ion source is located at the first floor 5.5 m upward the cyclotron median plane. The injection system consists of three sets of focusing elements, and a pair of electric deflector. The focusing element is a triplet of electric quadrupole lenses.

The injected beam is inflected by a electric mirror located at the center of the cyclotron. The injection system is equipped with following beam monitors; a pair of beam profile monitors, two sets of beam viewers, and two beam cups. A test for injecting polarized protons has been carried out. A beam buncher and a velocity selector are designed, and will be installed soon.

### 8. Control System

The cyclotron is controlled either by manual operator console with digital settings of operation parameters or by a computer. Initially controls of many devices are performed manually, but computer is partly used to preset, monitor and display operational parameters and status.

Stepping motor actuated potentiometers are used for setting of all power supplies. There is a 128-word core memory in a digital control system, and previous values of setting parameters are stored in the memory. This system consists of eight blocks and each block has 16 devices driven by stepping motors. If one device in a block is selected, the content of the corresponding memory address is loaded to a counter which is used to count number of pulses for stepping motor. After setting the number of pulses to the register by computer, the stepping motor is driven until the content of the counter gets equal to that of the register. Each block has a register and a counter for stepping motor drive, and can drive each stepping motor independently. Eight stepping motors are driven simultaneously, and 128 devices are controlled by this system. In the case of manual operator console thumbwheel switches are used instead of registers. When an operator selects one device by pushbutton, the counter is connected to the thumbwheel switch and the device can be controlled manually.

The control computer is PDP 11/40. It consists of 32 k words of core memory, typewriter, three 2.4 M byte cartridge disk units, a high speed paper tape reader and puncher, and two graphic displays. PDP 11/40 is connected to a host computer TOSBAC 5600/120. It has 128 k word memory, a card reader, a line printer, two 100 M byte disk units and two magnetic tape units. A simplified schematic diagram of computer control system is shown in fig. 5.

Contact closure output signals (up to 256) are used for the operations of power supplies. Contact sensor input signals (up to 768) are used to monitor the operational status of the devices. High resolution analog data (up to 16) are ADC readings acquired from main field, dee voltage and deflector voltages. Medium resolution analog data (up to 128) are also ADC readings from coil currents, power supply voltages and currents, and beam currents. For the setting of the frequency synthesizer which drives the RF system a 32-bit output register is used.

The computer and accelerator interface have been installed before this spring. Trim coils are operated using the computer control. Many devices are now under manual control, and they are in the stage of program development and operational tests of computer controls.

### 9. Extraction System

Two sets of a 52° wide electro-static deflector system are followed by a magnetic focus element and a magnetic weakening channel. The entrance septum for the first deflector system is fabricated from a 1.5 mm thick tungsten plate. The tungsten plate is partially scraped to 0.3 mm thick around the median plane. The V-slot is not cut on the entrance of the first septum. A pilot-septum (0.1 mm thick tungsten plate 24 mm in length) is located about 12 cm upstream of the first septum, and inclined at 2° to

the final orbit. The pilot-septum is designed to measure the position of the final orbit and to reduce local heating in the entrance septum with multiple scattering. The final half part of the second deflector system forms an electro-static quadrupole lens. The septum, the deflector and adjusting mechanisms of the gap are mounted on a plate. The position of the septum and the deflector gap can be adjusted independently.

### 10. Operation of the Cyclotron

Most of the beam measurements are made with alpha particles and low energy protons. To avoid the problem due to the residual radioactivity, the beam intensity is kept low using the ion source with a small exit slit (2 mm in diameter).

The internal beam has been tested with 20 MeV protons, and 60 MeV, 90 MeV and 120 MeV alpha particles. For alpha particles the maximum current of 25  $\mu$ A was obtained at full cyclotron radius of 100 cm. All settings of the trim coils except the center coil (No. 1 coil) are kept at the values given by the computer results through the measurements. So far the operating conditions are so adjusted to give about same number of turns which are expected for full energy protons. The beam is measured using four probes. The vertical motion, beam centering and turn pattern have been observed. The beam is very stable and reproducible. The current stability of internal beam is less than 1% for 10 min.

A 90 MeV alpha beam was extracted and the emittance was measured. The preliminary results show the vertical and horizontal emittances are less than 20 mm-mr and 40 mm-mr, respectively. An example of the measurements is shown in fig. 6.

### Acknowledgments

The authors wish to thank profs. H. Ikegami, H. Ogata and K. Nishimura, Dr. I. Katayama and Mr. M. Fujiwara for many helpful discussions, and Profs. T. Wakatsuki and K. Sugimoto for their encouragements. They also thank Prof. H. E. Conzett and the Berkeley cyclotron group for many suggestions.

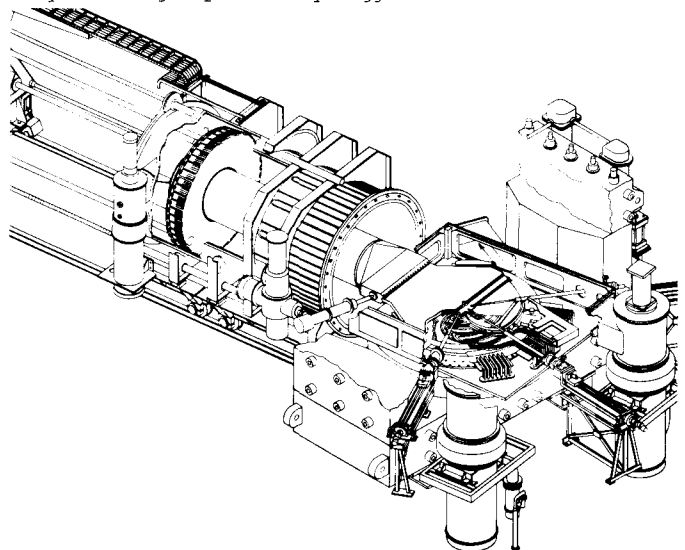


Fig. 1. Schematic view of the cyclotron

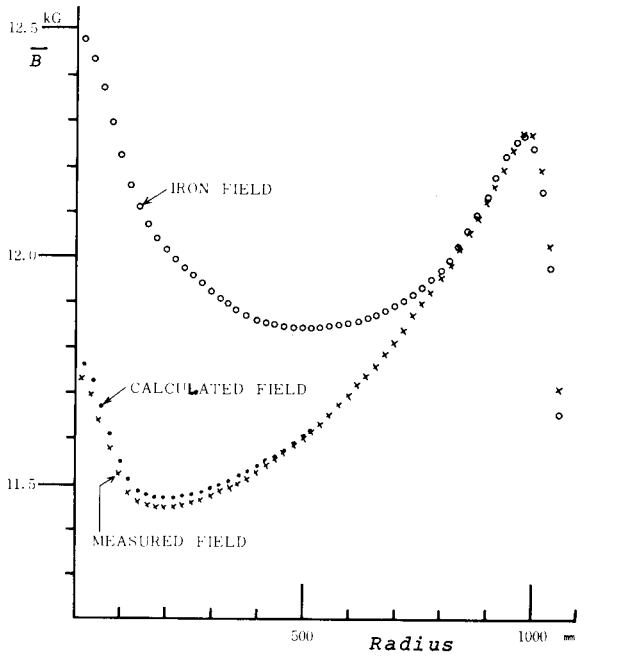


Fig. 2. Radial profile of the magnetic field. Discrepancy between the calculated and measured fields is caused by ignorance of change of central shim configuration in the calculated field

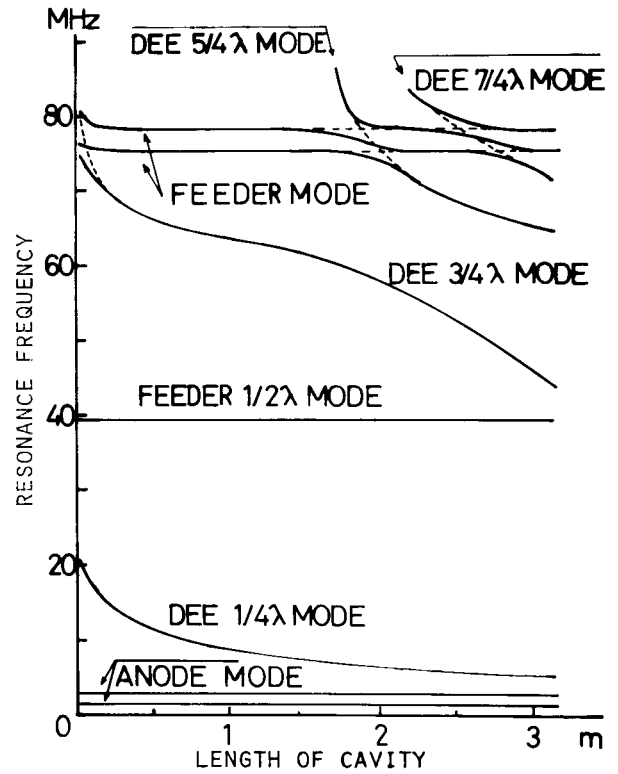


Fig. 4. Resonance frequency observed at the anode of the final amplifier

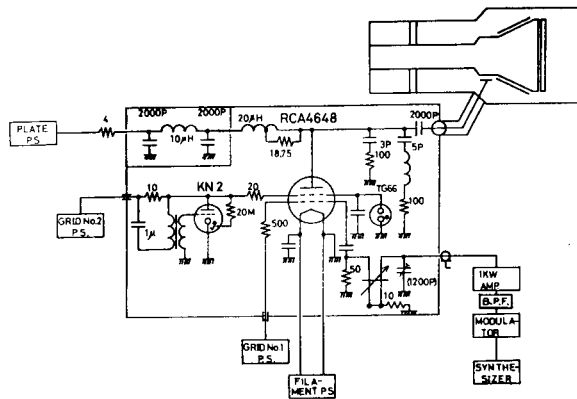


Fig. 3. Schematic diagram of the MOPA system.

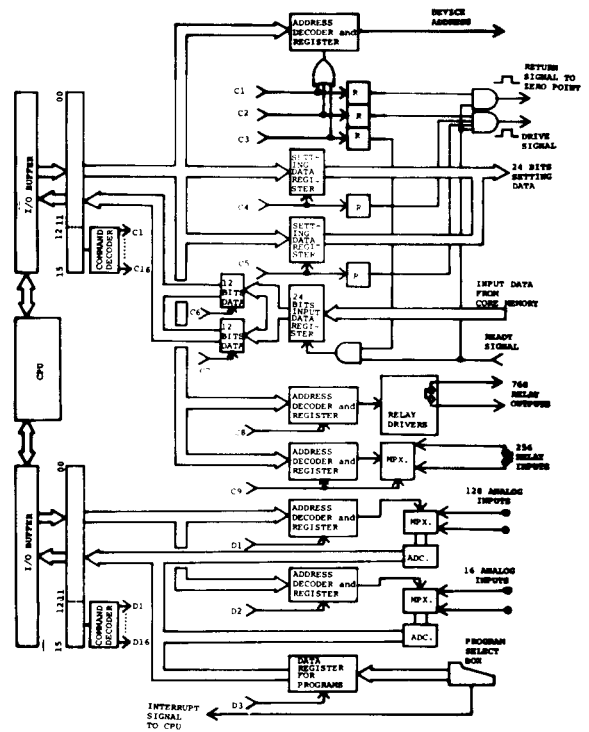


Fig. 5. Simplified schematic diagram of the computer control system

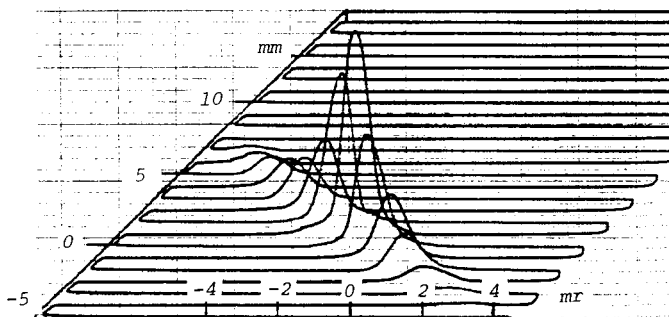


Fig. 6. Example of vertical emittance measurements